AIAA JOURNAL
Vol. 41, No. 11, November 2003

Vibration Analysis of Composite Wing Structures by a Matrix Form Comprehensive Model

Chyanbin Hwu* and H. S. Gai†
National Cheng-Kung University, Tainan 701, Taiwan, Republic of China

A dynamic model for stiffened composite multicell wing structures is developed. In this model, the extensional, bending, and coupling stiffnesses are calculated not only from the properties of the composite laminates of the wing skin but also from the stringers and spar flanges, which are treated as fibers of a pseudolamina. The arrangement of the wing spar webs and ribs is then treated like a sandwich honeycomb core, from which an equivalent transverse shear modulus of the wing structures is calculated. With these estimated properties, the composite wing structure is modeled, incorporating the effects of bending–torsion coupling, warping restraint, transverse shear deformation, shape of airfoil, rotary inertia, etc. To avoid complexity of formulation, the matrix form representation is introduced, which then makes most of the equations for the vibration analysis bear the same form as those of the classical beam theory. Thus, by following the classical approach, the composite wing structures can be studied analytically.

Nomenclature

A	=	area
A_{ij}, B_{ij}, D_{ij}	=	extensional, coupling, and bending stiffness
B_f	=	shape of β_f defined in Eq. (18)
B_r	=	shape of β_r defined in Eq. (18)
c	=	chordwise length
$\boldsymbol{D}$	=	coefficient matrix defined in Eq. (24b)
$\bar{D}_{ij}$, $\bar{D}^{*}_{ij}$, $\bar{D}^{**}_{ij}$	=	reduced bending stiffnesses defined in Eq. (17)
$\boldsymbol{d}$	=	coefficient vector defined in Eq. (20)
E	=	Young's modulus
$\boldsymbol{F}$, $\boldsymbol{F}_0$	=	force vector defined in Eqs. (13e) and (13f)
$f_u(\bar{x})$, $f_l(\bar{x})$	=	functions for the airfoil
G	=	shear modulus
h	=	thickness
$\boldsymbol{I}_0$	=	mass matrix defined in Eq. (13l) or Eq. (16f)
I_x, I_y, I_{xz}	=	moment of inertia
$\boldsymbol{K}_0$, $\boldsymbol{K}_1$, $\boldsymbol{K}_2$	=	stiffness matrices defined in Eqs. (13i–13k) or Eqs. (16c–16e)
$\boldsymbol{k}$	=	coefficient vector defined in Eq. (24c)
L	=	spanwise length
M_x, M_y, M_{xy}	=	bending moments
m	=	mass per unit spanwise length
m_x, m_y	=	distributed moments
N_j	=	generalized force
N_x, N_y, N_{xy}	=	in-plane forces
$\boldsymbol{p}$	=	vector of distributed loads defined in Eq. (13g) or Eq. (16b)
p_x, p_y, p	=	distributed loads
Q_x, Q_y	=	transverse shear forces
$\bar{Q}_{ij}$	=	transformed reduced stiffness
t	=	time
u, v, w	=	displacements
V_0	=	shape of v_0 defined in Eq. (18)
W	=	beam width
W_f	=	shape of w_f defined in Eq. (18)
x, y, z	=	coordinate system
x_c, z_c	=	center of gravity
z_k	=	location of the bottom surface of the kth lamina
α	=	transverse shear correction factor
β	=	rotation angle
β_r	=	rate of angle change in the x direction
γ_{xy}, γ_{xz}, γ_{yz}	=	shear strains
$\boldsymbol{\Delta}$	=	displacement vector defined in Eq. (18b)
$\boldsymbol{\delta}$	=	displacement vector defined in Eq. (13h) or Eq. (16a)
δ_{ij}	=	Kronecker delta
ε_x, ε_y	=	normal strains
$\eta_j(t)$	=	time-dependent generalized coordinate
Θ	=	shape of θ defined in Eq. (18)
θ	=	rotation angle with respect to x axis
λ	=	warping index
ν	=	Poisson's ratio
ρ	=	mass density
ω	=	natural frequency
$\langle\ \rangle$	=	diagonal matrix

Subscripts

0	=	midplane value
c	=	core
f	=	reference axis for w and β; or sandwich face for ρ and h; or spar flanges for other symbols
i, j, k	=	integer number
L	=	longitudinal direction
p	=	pseudolamina
s	=	stringer
T	=	transverse direction
w	=	wing cross section
x	=	x direction
y	=	y direction
z	=	z direction

Superscripts

T	=	transpose
$*$	=	multiplication by x
$\hat{}$	=	prescribed value
$\sim$	=	integration with respect to x
$'$	=	differentiation with respect to y
$\cdot$	=	time derivative

Received 14 November 2002; revision received 24 April 2003; accepted for publication 7 May 2003.

*Professor, Institute of Aeronautics and Astronautics.
†Graduate Student, Institute of Aeronautics and Astronautics.

I. Introduction

OVER the past five decades, several different structural models have been proposed to study composite wing structures, such as the classical beam model,[1,2] the coupled bending–torsion beam model (also called the box beam model),[3–5] and the

refined model considering warping restraint[6–9] and/or transverse shear deformation[10] and/or shell bending strain,[11,12] and/or cross-sectional materials and geometries,[13,14] etc.[15–18] A review of such literature before 1988 may be found in Ref. 19, whereas the most recent reviews of the composite beam modeling have been given by Jung et al.[20] and Volovoi et al.[21] For an improved prediction for the mechanical behavior of the stiffened composite multicell wing structures, a comprehensive refined model incorporating the various elastic and structural couplings, the warping restraint, the transverse shear deformation, the shape of airfoil effects, and so on, should naturally be a better choice for structural analysis. However, as may be expected, the more comprehensive the model is, the more difficult to obtain meaningful and useful analytical results. Hence, even though a comprehensive model was proposed around 10 years ago, most of the analytical work of wing structural analysis still uses the box beam model if the ignored effects will not induce drastic change of the results. To benefit from the accuracy of the comprehensive model as well as the simplicity of the classical beam model, in this paper we rederive the comprehensive model into a simple and elegant form by using the matrix form representation. Because of its simplicity, the vibration analysis by the comprehensive model, which is expected to be complicated, now becomes as simple as that of the classical beam model.

To show the accuracy and generality of the comprehensive dynamic model for the vibration analysis of stiffened composite multicell wing structures, several illustrative examples are given, such as a bending–torsion coupled cantilever composite beam, a cantilever composite sandwich beam, and a NACA 2412 composite wing. Moreover, the influential factors on the natural frequencies, such as the transverse shear deformation, warping restraint, and shape of the airfoil are all studied by this unified and general formulation. An example for the forced vibration analysis is then given by the vibration suppression of a composite wing with piezoelectric sensors and actuators bonded on the wing surfaces, for which a linear quadratic Gaussian/loop transfer recovery (LQG/LTR) controller is designed and proved to be successful for vibration suppression of composite wings.

II. Matrix Form Comprehensive Model for Composite Wing Structures

The primary function of the wing structure is providing the lift for an aircraft, which is governed by aerodynamic consideration. In addition to aerodynamic pressure, there are other forces resisted by the wing structures such as the weight of the structures, fuels, engines, undercarriage system, and/or possible carried weapons and the thrust of engines, etc. To sustain these loads, the wing structures usually consist of axial members in stringers, bending members in spars, shear panels in the cover skin and spar webs, and planar members in ribs. If the cover skin of the wing is made of composite laminates, the entire wing structure may be simulated by a composite sandwich plate in which the wing skins and stringers (including the spar flanges) are simulated as the faces, whereas the spar webs and ribs are simulated as the core of the sandwiches. Because the wing cross section must have a streamline shape commonly referred to as an airfoil section, the thickness of the sandwich will not be a constant but a function of the airfoil. Moreover, as with usual sandwich assumptions, the thickness is not too small to neglect the transverse shear deformation. Based on these considerations, a mathematical model for composite sandwich plates[22,23] has been applied by Hwu and Tsai[18] to model the stiffened composite multicell wing structures.

Because of the closely spaced stringers and the transverse stiffening members, such as wing spars and ribs, in aircraft analysis it is usually assumed that the wing chordwise section is rigid.[2] The displacement field consistent with the chordwise-rigid postulation and the basic assumptions for the composite sandwich plates can be written as[18]

$$u(x, y, z, t) = z\theta(y, t)$$
$$v(x, y, z, t) = v_0(y, t) + z\{\beta_f(y, t) + x\beta_r(y, t)\}$$
$$w(x, y, z, t) = w_f(y, t) - x\theta(y, t) \tag{1}$$

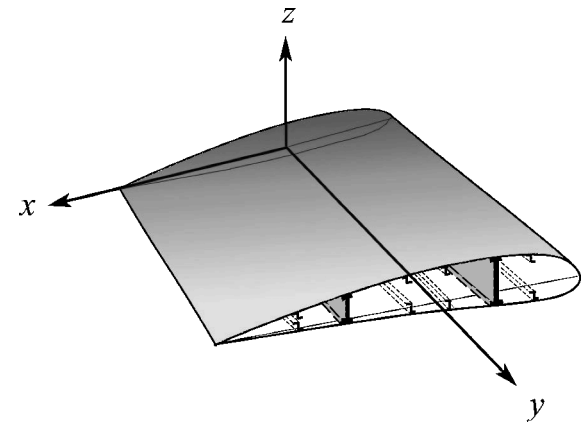

Fig. 1 Geometry of composite wing structures.

where u, v, and w are the displacement components in the directions of x (chordwise), y (spanwise), and z (thicknesswise), respectively (Fig. 1). Here t is the time variable, v_0 the midplane displacement in the y direction, w_f the deflection (positive upward) measured at the line of the reference axis, and θ the rotation angle with respect to x axis due to the twist around the reference axis (positive nose up), that is, $\beta_x = \theta$. Also, β_f is the rotation angle with respect to the y axis measured at the reference axis. Thus, $\beta_y = \beta_f + x\beta_r$. By the assumption in Eq. (1), the strains in the stiffened composite wings can be expressed as

$$\varepsilon_x = 0, \qquad \varepsilon_y = v_0' + z(\beta_f' + \lambda x\beta_r'), \qquad \gamma_{xy} = z(\beta_r + \theta')$$
$$\gamma_{xz} = 0, \qquad \gamma_{yz} = \beta_f + w_f' + x(\beta_r - \theta') \tag{2}$$

where the prime indicates differentiation with respect to y. Notice that a tracer λ has been included in the coefficient of $x\beta_r'$ of ε_y of Eq. (2) to identify the warping effect. Here λ takes the value 0 or 1, according to whether the free warping or warping restraint is implied, respectively.[15]

According to the postulation in Eq. (1), the basic functions describing the deformation of the stiffened composite wing structures become v_0, w_f, θ, β_f, and β_r. To find the equations of motion corresponding to these basic functions, we first consider the equations of motions for composite sandwich plates, which can be expressed in terms of the stress resultants, N_x, N_y, N_{xy}, Q_x, and Q_y, and bending moments, M_x, M_y, and M_{xy}, as

$$\frac{\partial N_x}{\partial x} + \frac{\partial N_{xy}}{\partial y} + p_x = \int_{z_l}^{z_u} \rho\ddot{u}\,\mathrm{d}z$$
$$\frac{\partial N_{xy}}{\partial x} + \frac{\partial N_y}{\partial y} + p_y = \int_{z_l}^{z_u} \rho\ddot{v}\,\mathrm{d}z$$
$$\frac{\partial Q_x}{\partial x} + \frac{\partial Q_y}{\partial y} + p = \int_{z_l}^{z_u} \rho\ddot{w}\,\mathrm{d}z$$
$$\frac{\partial M_x}{\partial x} + \frac{\partial M_{xy}}{\partial y} - Q_x + m_x = \int_{z_l}^{z_u} \rho\ddot{u}z\,\mathrm{d}z$$
$$\frac{\partial M_{xy}}{\partial x} + \frac{\partial M_y}{\partial y} - Q_y + m_y = \int_{z_l}^{z_u} \rho\ddot{v}z\,\mathrm{d}z \tag{3}$$

where p_x, p_y, p and m_x, m_y are the total distributed loads and moments applied on the upper and lower surfaces of the sandwich plates and z_l and z_u are the locations of the upper and lower surfaces of the plates.

To obtain the equations of motion corresponding to the basic variables v_0, w_f, θ, β_f, and β_r, we now substitute Eq. (1) into

Eq. (3) and perform the integration with respect to x as follows:

$$\int (3)_2\,\mathrm{d}x, \qquad \int (3)_3\,\mathrm{d}x, \qquad \int [(3)_4 - x(3)_3]\,\mathrm{d}x$$

$$\int (3)_5\,\mathrm{d}x, \qquad \int (3)_5 x\,\mathrm{d}x$$

The results are

$$\frac{\partial \tilde{N}_y}{\partial y} + \tilde{p}_y = m\ddot{v}_0 + mz_c\ddot{\beta}_f + I_{xz}\ddot{\beta}_r \tag{4a}$$

$$\frac{\partial \tilde{Q}_y}{\partial y} + \tilde{p} = m\ddot{w}_f - mx_c\ddot{\theta} \tag{4b}$$

$$\frac{\partial\left(\tilde{M}_{xy} - \tilde{Q}^*_y\right)}{\partial y} + \tilde{m}_x - \tilde{p}^* = I_y\ddot{\theta} - mx_c\ddot{w}_f \tag{4c}$$

$$\frac{\partial \tilde{M}_y}{\partial y} - \tilde{Q}_y + \tilde{m}_y = mz_c\ddot{v}_0 + I_x\ddot{\beta}_f + I_{xz^2}\ddot{\beta}_r \tag{4d}$$

$$\lambda\frac{\partial \tilde{M}^*_y}{\partial y} - \tilde{M}_{xy} - \tilde{Q}^*_y + \tilde{m}^*_y = I_{xz}\ddot{v}_0 + I_{xz^2}\ddot{\beta}_f + I_{x^2z^2}\ddot{\beta}_r \tag{4e}$$

where (x_c, z_c) is the coordinate of the center of gravity and I is the mass moment of inertia defined by

$$m = \int_A \rho\,\mathrm{d}A, \qquad mx_c = \int_A \rho x\,\mathrm{d}A, \qquad mz_c = \int_A \rho z\,\mathrm{d}A$$

$$I_x = \int_A \rho z^2\,\mathrm{d}A, \qquad I_y = \int_A \rho(x^2 + z^2)\,\mathrm{d}A$$

$$I_{xz} = \int_A \rho xz\,\mathrm{d}A, \qquad I_{xz^2} = \int_A \rho xz^2\,\mathrm{d}A$$

$$I_{x^2z^2} = \int_A \rho x^2z^2\,\mathrm{d}A \tag{5}$$

where A is the area of chordwise cross section. Note that in this paper, the tilde $\sim$ and the superscript asterisk denote, respectively, integration with respect to x and multiplication by x, for example,

$$\tilde{M}_y = \int M_y\,\mathrm{d}x, \qquad \tilde{M}^*_y = \int x\tilde{M}_y\,\mathrm{d}x, \qquad \tilde{Q}^*_y = \int x\tilde{Q}_y\,\mathrm{d}x \tag{6}$$

In our previous study for static modeling,[18] we found that the force terms corresponding to the basic variables v_0, w_f, θ, β_f, and β_r are $\tilde{N}_y$, $\tilde{Q}_y$, $\tilde{M}_{xy} - \tilde{Q}^*_y$, $\tilde{M}_y$, and $\tilde{M}^*_y$. In a way similar to classical lamination theory, the constitutive relations between the basic variables and their corresponding forces can be written as[18]

$$\tilde{N}_y = \tilde{A}_{22}v_0' + \tilde{B}_{22}\beta_f' + \tilde{B}^*_{22}\lambda\beta_r' + \tilde{B}_{26}(\beta_r + \theta') \tag{7a}$$

$$\tilde{M}_y = \tilde{B}_{22}v_0' + \tilde{D}_{22}\beta_f' + \tilde{D}^*_{22}\lambda\beta_r' + \tilde{D}_{26}(\beta_r + \theta') \tag{7b}$$

$$\tilde{M}_{xy} = \tilde{B}_{26}v_0' + \tilde{D}_{26}\beta_f' + \tilde{D}^*_{26}\lambda\beta_r' + \tilde{D}_{66}(\beta_r + \theta') \tag{7c}$$

$$\tilde{Q}^*_y = \tilde{A}^*_{44}(\beta_f + w_f') + \tilde{A}^{**}_{44}(\beta_r - \theta') \tag{7d}$$

$$\tilde{Q}_y = \tilde{A}_{44}(\beta_f + w_f') + \tilde{A}^*_{44}(\beta_r - \theta') \tag{7e}$$

$$\tilde{M}^*_y = \tilde{B}^*_{22}v_0' + \tilde{D}^*_{22}\beta_f' + \tilde{D}^{**}_{22}\lambda\beta_r' + \tilde{D}^*_{26}(\beta_r + \theta') \tag{7f}$$

where

$$\tilde{A}_{ij} = \int_{-c/2}^{c/2} A_{ij}\,\mathrm{d}x, \qquad \tilde{B}_{ij} = \int_{-c/2}^{c/2} B_{ij}\,\mathrm{d}x, \qquad \tilde{D}_{ij} = \int_{-c/2}^{c/2} D_{ij}\,\mathrm{d}x$$

$$\tilde{A}^*_{ij} = \int_{-c/2}^{c/2} A_{ij}x\,\mathrm{d}x, \qquad \tilde{B}^*_{ij} = \int_{-c/2}^{c/2} B_{ij}x\,\mathrm{d}x$$

$$\tilde{D}^*_{ij} = \int_{-c/2}^{c/2} D_{ij}x\,\mathrm{d}x$$

$$\tilde{A}^{**}_{ij} = \int_{-c/2}^{c/2} A_{ij}x^2\,\mathrm{d}x, \qquad \tilde{B}^{**}_{ij} = \int_{-c/2}^{c/2} B_{ij}x^2\,\mathrm{d}x$$

$$\tilde{D}^{**}_{ij} = \int_{-c/2}^{c/2} D_{ij}x^2dx, \qquad i, j = 1, 2, \ldots, 6 \tag{8}$$

and A_{ij}, B_{ij}, and D_{ij} are the extensional, coupling and bending stiffnesses, respectively, which are defined by

$$A_{44} = \alpha h G_{yz}, \qquad A_{ij} = \sum_{k=1}^{n} (\bar{Q}_{ij})_k (z_k - z_{k-1})$$

$$B_{ij} = \frac{1}{2}\sum_{k=1}^{n} (\bar{Q}_{ij})_k \left(z_k^2 - z_{k-1}^2\right)$$

$$D_{ij} = \frac{1}{3}\sum_{k=1}^{n} (\bar{Q}_{ij})_k \left(z_k^3 - z_{k-1}^3\right), \qquad i, j = 1, 2, 6 \tag{9}$$

In Eq. (9), h is the thickness of the wing cross section and is a function of x, G_{yz} is the transverse shear modulus in y–z plane, and α is selected to be five-sixths for the present case.[24] $(\bar{Q}_{ij})_k$ are the transformed reduced stiffnesses of the kth lamina, and z_k and z_{k-1} are the location of the bottom and top surfaces of the kth lamina, respectively.

Note that in the calculation of A_{ij}, B_{ij}, and D_{ij}, not only the composite laminates of the faces are counted but also the stringers and spar flanges, which are considered to be the fibers of a pseudolamina. The equivalent material properties of this pseudolamina can be found by the rule of mixture as[18]

$$E_L = E_s(A_s/A_p) + E_f(A_f/A_p)$$

$$\nu_{LT} = \nu_s(A_s/A_p) + \nu_f(A_f/A_p), \qquad E_T = 0, \qquad G_{LT} = 0 \tag{10}$$

where A is the cross-sectional area. The subscript f denotes the spar flange, and A_p is the cross-sectional area of the pseudolamina.

To find a proper transverse shear modulus G_{yz} that may represent the shear resistance of the multicellular wing structures, the arrangement of the wing spar webs and ribs can be treated like a sandwich honeycomb core. When uniform transverse shear strain is assumed over the wing cross section, the equivalent transverse shear modulus G_{yz} can be estimated by[18]

$$G_{yz} = \sum_{k=1}^{n_s} G_k\frac{A_k}{A_w} \tag{11}$$

where G_k and A_k are the shear modulus and section area of the kth spar web, A_w is the wing cross-sectional area, and n_s is the number of the wing spars.

Because the independent variables for the displacements and forces are v_0, w_f, θ, β_f, and β_r, and $\tilde{N}_y$, $\tilde{Q}_y$, $\tilde{M}_{xy} - \tilde{Q}^*_y$, $\tilde{M}_y$, and $\tilde{M}^*_y$, the boundary conditions along $y = \text{const}$ of the composite wing

can be expressed as[18]

$$\tilde{N}_y = \hat{\tilde{N}}_y, \quad \text{or} \quad v_0 = \hat{v}_0$$

$$\tilde{Q}_y = \hat{\tilde{Q}}_y, \quad \text{or} \quad w_f = \hat{w}_f$$

$$\tilde{M}_{xy} - \tilde{Q}^*_y = \hat{\tilde{M}}_{xy} - \hat{\tilde{Q}}^*_y, \quad \text{or} \quad \theta = \hat{\theta}$$

$$\tilde{M}_y = \hat{\tilde{M}}_y, \quad \text{or} \quad \beta_f = \hat{\beta}_f$$

$$\lambda\tilde{M}^*_y = \lambda\hat{\tilde{M}}^*_y, \quad \text{or} \quad \lambda\beta_r = \lambda\hat{\beta}_r \tag{12}$$

By using the constitutive relations given in Eq. (7), the equations of motion (4) can be expressed in terms of five basic unknown functions, v_0, w_f, θ, β_f, and β_r, that constitute a 10th-order system of five partial differential equations. This system of equations can be completely solved with 10 boundary conditions (12) together with 10 initial conditions, which consist of five conditions per each edge and two conditions at $t = 0$ for each basic function. Because of the complexity of the equations, in most papers, the final governing equations are not expressed in detail or their associated problems are not expressed in general. Here detailed expressions will be given in a compact matrix form, and then associated problems will be solved by analogy with the scalar form expressions. With this understanding, we now rewrite the equations of motion (4), constitutive relations (7), and boundary conditions (12) as follows:

$$\boldsymbol{F}' - \boldsymbol{F}_0 + \boldsymbol{p} = \boldsymbol{I}_0\ddot{\boldsymbol{\delta}} \tag{13a}$$

$$\boldsymbol{F} = \boldsymbol{K}_1\boldsymbol{\delta} + \boldsymbol{K}_2\boldsymbol{\delta}' \tag{13b}$$

$$\boldsymbol{F}_0 = \boldsymbol{K}_0\boldsymbol{\delta} + \boldsymbol{K}_1^T\boldsymbol{\delta}' \tag{13c}$$

$$\boldsymbol{F} = \hat{\boldsymbol{F}}, \quad \text{or} \quad \boldsymbol{\delta} = \hat{\boldsymbol{\delta}} \quad \text{along } y = \text{const} \tag{13d}$$

where

$$\boldsymbol{F} = \begin{Bmatrix} \tilde{N}_y \\ \tilde{Q}_y \\ \tilde{M}_{xy} - \tilde{Q}^*_y \\ \tilde{M}_y \\ \lambda\tilde{M}^*_y \end{Bmatrix} \tag{13e}$$

$$\boldsymbol{F}_0 = \begin{Bmatrix} 0 \\ 0 \\ 0 \\ \tilde{Q}_y \\ \tilde{M}_{xy} + \tilde{Q}^*_y \end{Bmatrix} \tag{13f}$$

$$\boldsymbol{p} = \begin{Bmatrix} \tilde{p}_y \\ \tilde{p} \\ \tilde{m}_x - \tilde{p}^* \\ \tilde{m}_y \\ \tilde{m}^*_y \end{Bmatrix} \tag{13g}$$

$$\boldsymbol{\delta} = \begin{Bmatrix} v_0 \\ w_f \\ \theta \\ \beta_f \\ \beta_r \end{Bmatrix} \tag{13h}$$

$$\boldsymbol{K}_2 = \begin{bmatrix} \tilde{A}_{22} & 0 & \tilde{B}_{26} & \tilde{B}_{22} & \lambda\tilde{B}^*_{22} \\ 0 & \tilde{A}_{44} & -\tilde{A}^*_{44} & 0 & 0 \\ \tilde{B}_{26} & -\tilde{A}^*_{44} & \tilde{D}_{66} + \tilde{A}^{**}_{44} & \tilde{D}_{26} & \lambda\tilde{D}^*_{26} \\ \tilde{B}_{22} & 0 & \tilde{D}_{26} & \tilde{D}_{22} & \lambda\tilde{D}^*_{22} \\ \lambda\tilde{B}^*_{22} & 0 & \lambda\tilde{D}^*_{26} & \lambda\tilde{D}^*_{22} & \lambda\tilde{D}^{**}_{22} \end{bmatrix} \tag{13i}$$

$$\boldsymbol{K}_1 = \begin{bmatrix} 0 & 0 & 0 & 0 & \tilde{B}_{26} \\ 0 & 0 & 0 & \tilde{A}_{44} & \tilde{A}^*_{44} \\ 0 & 0 & 0 & -\tilde{A}^*_{44} & \tilde{D}_{66} - \tilde{A}^{**}_{44} \\ 0 & 0 & 0 & 0 & \tilde{D}_{26} \\ 0 & 0 & 0 & 0 & \lambda\tilde{D}^*_{26} \end{bmatrix} \tag{13j}$$

$$\boldsymbol{K}_0 = \begin{bmatrix} 0 & 0 & 0 & 0 & 0 \\ 0 & 0 & 0 & 0 & 0 \\ 0 & 0 & 0 & 0 & 0 \\ 0 & 0 & 0 & \tilde{A}_{44} & \tilde{A}^*_{44} \\ 0 & 0 & 0 & \tilde{A}^*_{44} & \tilde{D}_{66} + \tilde{A}^{**}_{44} \end{bmatrix} \tag{13k}$$

$$\boldsymbol{I}_0 = \begin{bmatrix} m & 0 & 0 & mz_c & I_{xz} \\ 0 & m & -mx_c & 0 & 0 \\ 0 & -mx_c & I_y & 0 & 0 \\ mz_c & 0 & 0 & I_x & I_{xz^2} \\ I_{xz} & 0 & 0 & I_{xz^2} & I_{x^2z^2} \end{bmatrix} \tag{13l}$$

Substituting Eqs. (13b) and (13c) into Eq. (13a), we can then write the governing equations for the stiffened composite wing structures in terms of the basic function vector $\boldsymbol{\delta}$ as

$$\boldsymbol{K}_2\boldsymbol{\delta}''(y,t) + \left(\boldsymbol{K}_1 - \boldsymbol{K}_1^T\right)\boldsymbol{\delta}'(y,t) - \boldsymbol{K}_0\boldsymbol{\delta}(y,t) + \boldsymbol{p}(y,t) = \boldsymbol{I}_0\ddot{\boldsymbol{\delta}}(y,t) \tag{14}$$

If the wing is fixed at the root ($y = 0$) and free at the tip ($y = L$), by Eqs. (13d), the boundary conditions of the wing structures can now be written as

$$\boldsymbol{\delta}(0) = \boldsymbol{0}, \qquad \boldsymbol{K}_1\boldsymbol{\delta}(L) + \boldsymbol{K}_2\boldsymbol{\delta}'(L) = \boldsymbol{0} \tag{15}$$

If the influence of the in-plane spanwise surface loads $\tilde{p}_y$, as well as of in-plane and rotary inertia terms $m\ddot{v}_0$, $mz_c\ddot{\beta}_f$, and $I_{xz}\ddot{\beta}_r$, can be disregarded, the first equation of motion (4a) will lead to $\tilde{N}_y = \text{const}$. If no in-plane spanwise loads are applied at the wingtip, this constant value will then be identical to zero, that is, $\tilde{N}_y = 0$ along the entire wing. When this result is substituted into constitutive relations (7a–7f), v_0' may be expressed in terms of β_f', β_r', and $\beta_r + \theta'$. Thus, the 10th-order system of equations can be reduced to an equivalent eighth-order system of equations, which should bear exactly the same form as Eq. (14) except that the dimensions of $\boldsymbol{\delta}$ and $\boldsymbol{p}$ will be reduced to 4×1 and those of $\boldsymbol{K}_2$, $\boldsymbol{K}_1$, and $\boldsymbol{K}_0$ to 4×4 as

$$\boldsymbol{\delta}(y,t) = \begin{Bmatrix} w_f(y,t) \\ \theta(y,t) \\ \beta_f(y,t) \\ \beta_r(y,t) \end{Bmatrix} \tag{16a}$$

$$\boldsymbol{p} = \begin{Bmatrix} \tilde{p} \\ \tilde{m}_x - \tilde{p}^* \\ \tilde{m}_y \\ \tilde{m}^*_y \end{Bmatrix} \tag{16b}$$

$$\boldsymbol{K}_2 = \begin{bmatrix} \tilde{A}_{44} & -\tilde{A}^*_{44} & 0 & 0 \\ -\tilde{A}^*_{44} & \bar{D}_{66} + \tilde{A}^{**}_{44} & \bar{D}_{26} & \lambda\bar{D}^*_{26} \\ 0 & \bar{D}_{26} & \bar{D}_{22} & \lambda\bar{D}^*_{22} \\ 0 & \lambda\bar{D}^*_{26} & \lambda\bar{D}^*_{22} & \lambda\bar{D}^{**}_{22} \end{bmatrix} \tag{16c}$$

$$\boldsymbol{K}_1 = \begin{bmatrix} 0 & 0 & \tilde{A}_{44} & \tilde{A}^*_{44} \\ 0 & 0 & -\tilde{A}^*_{44} & \bar{D}_{66} - \tilde{A}^{**}_{44} \\ 0 & 0 & 0 & \bar{D}_{26} \\ 0 & 0 & 0 & \lambda\bar{D}^*_{26} \end{bmatrix} \tag{16d}$$

$$\boldsymbol{K}_0 = \begin{bmatrix} 0 & 0 & 0 & 0 \\ 0 & 0 & 0 & 0 \\ 0 & 0 & \tilde{A}_{44} & \tilde{A}^*_{44} \\ 0 & 0 & \tilde{A}^*_{44} & \bar{D}_{66} + \tilde{A}^{**}_{44} \end{bmatrix} \tag{16e}$$

$$\boldsymbol{I}_0 = \begin{bmatrix} m & -mx_c & 0 & 0 \\ -mx_c & I_y & 0 & 0 \\ 0 & 0 & 0 & 0 \\ 0 & 0 & 0 & 0 \end{bmatrix} \tag{16f}$$

In Eqs. (16), $\bar{D}_{ij}$, $\bar{D}^*_{ij}$, and $\bar{D}^{**}_{ij}$ are defined by

$$\bar{D}_{ij} = \tilde{D}_{ij} - \tilde{B}_{i2}\tilde{B}_{2j}/\tilde{A}_{22}, \qquad \bar{D}^*_{ij} = \tilde{D}^*_{ij} - \tilde{B}^*_{i2}\tilde{B}_{2j}\big/\tilde{A}_{22}$$

$$\bar{D}^{**}_{ij} = \tilde{D}^{**}_{ij} - \tilde{B}^*_{i2}\tilde{B}^*_{2j}\big/\tilde{A}_{22}, \qquad i, j = 2, 6 \tag{17}$$

Because the displacement fields assumed in Eq. (1) are quite general, several special conditions considered in the literature can be covered by the present formulations. For example, 1) neglect of the transverse shear deformation can be formulated by letting $\gamma_{yz} = 0$, which will lead to $\beta_f = -w'_f$ and $\beta_r = \theta'$; 2) neglect of the warping restraint effect can be formulated by letting $\varepsilon_y = v'_0 + z\beta'_f$, which will lead to $\lambda = 0$; 3) reduction to the conventional composite sandwich beams can be formulated by letting $\theta = \beta_r = 0$; and 4) reduction of conventional laminated beams can be formulated by letting $\theta = \beta_r = 0$, $\beta_f = -w'_f$, and $I_x = 0$. Detailed derivations of the reduction of our general formulations to these special cases are presented in the Appendix.

III. Vibration Analysis

Free Vibration

To determine the natural frequency and its associated vibration mode of the stiffened composite wing structures, we consider the case that the external forces $\tilde{p}$ and $\tilde{p}_y$, torsional moment $\tilde{p}^*$, and the distributed moments $\tilde{m}_x$, $\tilde{m}_y$, and $\tilde{m}^*_y$ are all zero, that is, the force vector $\boldsymbol{p} = \boldsymbol{0}$ in Eq. (13g). To find the natural modes of vibration, the usual way is the method of separation of variables. By this method we write the deflection $\boldsymbol{\delta}(y, t)$ as a product of a function $\boldsymbol{\Delta}(y)$ of the spatial variables only and a function $f(t)$ depending on time only. Furthermore, because of free vibration, $f(t)$ is harmonic and of frequency ω. Thus,

$$\boldsymbol{\delta}(y, t) = \boldsymbol{\Delta}(y)e^{i\omega t} \tag{18a}$$

where

$$\boldsymbol{\Delta}(y) = \begin{Bmatrix} V_0(y) \\ W_f(y) \\ \Theta(y) \\ B_f(y) \\ B_r(y) \end{Bmatrix} \tag{18b}$$

Through the use of Eq. (18), the equation of motion (14) can easily be reduced to a system of ordinary differential equations,

$$\boldsymbol{K}_2\boldsymbol{\Delta}''(y) + \left(\boldsymbol{K}_1 - \boldsymbol{K}_1^T\right)\boldsymbol{\Delta}'(y) - \boldsymbol{K}_0\boldsymbol{\Delta}(y) + \omega^2\boldsymbol{I}_0\boldsymbol{\Delta}(y) = \boldsymbol{0} \tag{19}$$

which can be solved by letting

$$\boldsymbol{\Delta}(y) = \boldsymbol{d}e^{ry} \tag{20}$$

Substituting Eq. (20) into Eq. (19), we get

$$\left\{\boldsymbol{K}_2 r^2 + \left(\boldsymbol{K}_1 - \boldsymbol{K}_1^T\right)r - \boldsymbol{K}_0 + \omega^2\boldsymbol{I}_0\right\}\boldsymbol{d} = \boldsymbol{0} \tag{21}$$

whose nonvanishing solutions exist only when the determinant of the coefficient matrix of $\boldsymbol{d}$ becomes zero, that is,

$$\left\|\boldsymbol{K}_2 r^2 + \left(\boldsymbol{K}_1 - \boldsymbol{K}_1^T\right)r - \boldsymbol{K}_0 + \omega^2\boldsymbol{I}_0\right\| = 0 \tag{22}$$

As shown in Eqs. (13i–13l), the coefficient matrix of $\boldsymbol{d}$ is a 5×5 matrix for the general cases. Thus, Eq. (22) is a 10th-order polynomial equation, which will have 10 roots, $r_i(\omega)$, $i = 1, 2, \ldots, 10$. Each of the roots has an associated eigenvector $\boldsymbol{d}_i(\omega)$ determined from Eq. (21). Linear superposition of these 10 homogeneous solutions now gives us

$$\boldsymbol{\Delta}(y) = \sum_{i=1}^{10} k_i\boldsymbol{d}_i e^{r_i y} \tag{23}$$

Substituting Eqs. (23) and (18) into the boundary conditions (15) will then set a system of 10 simultaneous linear algebraic equations with 10 unknown coefficients k_i as

$$\begin{bmatrix} \boldsymbol{K}_1\boldsymbol{D}\langle e^{r_i L}\rangle + \boldsymbol{K}_2\boldsymbol{D}\langle r_i e^{r_i L}\rangle \\ \boldsymbol{D} \end{bmatrix}\boldsymbol{k} = \boldsymbol{0} \tag{24a}$$

where

$$\boldsymbol{D} = [\boldsymbol{d}_1 \quad \boldsymbol{d}_2 \ldots \quad \boldsymbol{d}_{10}] \tag{24b}$$

$$\boldsymbol{k} = \begin{Bmatrix} k_1 \\ k_2 \\ \vdots \\ k_{10} \end{Bmatrix} \tag{24c}$$

and the angle brackets $\langle\,\rangle$ indicate a diagonal matrix in which each component is varied according to its subscript i, for example, $\langle r_i e^{r_i L}\rangle = \text{diag}\cdot[r_1 e^{r_1 L}, r_2 e^{r_2 L}, \ldots, r_{10} e^{r_{10} L}]$.

Because both the eigenvalues r_i and the eigenvectors $\boldsymbol{d}_i$ are functions of the natural frequency ω, the coefficient matrix of $\boldsymbol{k}$ in Eq. (24a) is a function of the natural frequency ω. Again, nonvanishing solutions exist only when the determinant of the coefficient matrix of $\boldsymbol{k}$ becomes zero, by which we can then obtain the natural frequencies of the stiffened composite wing structures. With the determined natural frequency ω, the coefficients k_i can be calculated from Eq. (24a) as the eigenvector, and hence, the natural vibration mode shapes of the composite wing structures are obtained from Eq. (23).

Orthogonality Condition

If the family of natural vibration mode shapes $\boldsymbol{\Delta}_j(y)$ can constitute a complete set of orthonormal modes, most of the vibration problems can be solved by modal analysis through the use of the expansion theorem.[25] Let ω_i and ω_j be the two distinct natural frequencies and $\boldsymbol{\Delta}_i(y)$ and $\boldsymbol{\Delta}_j(y)$ be the corresponding natural modes of vibration resulting from the solution of the equations of motion (19) and its associated boundary conditions (15). Consider Eq. (19) corresponding to ω_i and $\boldsymbol{\Delta}_i(y)$, and multiplied by $\boldsymbol{\Delta}_j^T(y)$, and another equation (19) corresponding to ω_j and $\boldsymbol{\Delta}_j(y)$, and multiplied by $\boldsymbol{\Delta}_i^T(y)$. Subtracting these two equations and integrating the results over the wing spanwise length L, we obtain

$$\left(\omega_i^2 - \omega_j^2\right)\int_0^L \boldsymbol{\Delta}_j^T\boldsymbol{I}_0\boldsymbol{\Delta}_i\,\mathrm{d}y$$

$$= \int_0^L \left(-\boldsymbol{\Delta}_j^T\boldsymbol{K}_0\boldsymbol{\Delta}_i + \boldsymbol{\Delta}_i^T\boldsymbol{K}_0\boldsymbol{\Delta}_j + \boldsymbol{\Delta}_j^T\left(\boldsymbol{K}_1 - \boldsymbol{K}_1^T\right)\boldsymbol{\Delta}'_i\right.$$

$$\left. - \boldsymbol{\Delta}_i^T\left(\boldsymbol{K}_1 - \boldsymbol{K}_1^T\right)\boldsymbol{\Delta}'_j + \boldsymbol{\Delta}_j^T\boldsymbol{K}_2\boldsymbol{\Delta}''_i - \boldsymbol{\Delta}_i^T\boldsymbol{K}_2\boldsymbol{\Delta}''_j\right)\mathrm{d}y \tag{25}$$

From Eqs. (13i–13l), we see that $\boldsymbol{K}_2$, $\boldsymbol{K}_0$, and $\boldsymbol{I}_0$ are symmetric matrices. Knowing that the transpose of a symmetric matrix (including a scalar) is identical to the matrix itself, we have

$$\boldsymbol{K}_2 = \boldsymbol{K}_2^T, \qquad \boldsymbol{K}_0 = \boldsymbol{K}_0^T, \qquad \boldsymbol{I}_0 = \boldsymbol{I}_0^T$$

$$\boldsymbol{\Delta}_j^T \boldsymbol{K}_0 \boldsymbol{\Delta}_i = \left(\boldsymbol{\Delta}_j^T \boldsymbol{K}_0 \boldsymbol{\Delta}_i\right)^T, \ldots \tag{26}$$

With relation (26), Eq. (25) can be further reduced to

$$\begin{aligned}
&\left(\omega_i^2 - \omega_j^2\right) \int_0^L \boldsymbol{\Delta}_j^T \boldsymbol{I}_0 \boldsymbol{\Delta}_i \, \mathrm{d}y \\
&= \int_0^L \left\{\left[\boldsymbol{\Delta}_j^T \left(\boldsymbol{K}_1 - \boldsymbol{K}_1^T\right)\boldsymbol{\Delta}_i\right]' + \boldsymbol{\Delta}_j^T \boldsymbol{K}_2 \boldsymbol{\Delta}_i'' - \boldsymbol{\Delta}_i^T \boldsymbol{K}_2 \boldsymbol{\Delta}_j''\right\} \mathrm{d}y \\
&= \boldsymbol{\Delta}_j^T \left(\boldsymbol{K}_1 - \boldsymbol{K}_1^T\right)\boldsymbol{\Delta}_i \Big|_0^L + \int_0^L \left\{\left(\boldsymbol{\Delta}_j^T \boldsymbol{K}_2 \boldsymbol{\Delta}_i'\right)'\right. \\
&\left. - \boldsymbol{\Delta}_j'^T \boldsymbol{K}_2 \boldsymbol{\Delta}_i' - \left(\boldsymbol{\Delta}_i^T \boldsymbol{K}_2 \boldsymbol{\Delta}_j'\right)' + \boldsymbol{\Delta}_i'^T \boldsymbol{K}_2 \boldsymbol{\Delta}_j'\right\} \mathrm{d}y \\
&= \left\{\boldsymbol{\Delta}_j^T \left(\boldsymbol{K}_1 \boldsymbol{\Delta}_i + \boldsymbol{K}_2 \boldsymbol{\Delta}_i'\right) - \boldsymbol{\Delta}_i^T \left(\boldsymbol{K}_1 \boldsymbol{\Delta}_j + \boldsymbol{K}_2 \boldsymbol{\Delta}_j'\right)\right\}\Big|_0^L \\
&= \left(\boldsymbol{\Delta}_j^T \boldsymbol{F}_i - \boldsymbol{\Delta}_i^T \boldsymbol{F}_j\right)\Big|_0^L
\end{aligned} \tag{27}$$

in which the last equality comes from Eqs. (13b) and (18). Because the boundary conditions are either displacement prescribed or force prescribed, we have

$$\begin{aligned}
\boldsymbol{F}(0) &= \boldsymbol{0}, \qquad \text{or} \qquad \boldsymbol{\Delta}(0) = \boldsymbol{0} \\
\boldsymbol{F}(L) &= \boldsymbol{0}, \qquad \text{or} \qquad \boldsymbol{\Delta}(L) = \boldsymbol{0}
\end{aligned} \tag{28}$$

Substituting Eq. (28) into Eq. (27) for both of the ith and jth modes, we get

$$\left(\omega_i^2 - \omega_j^2\right) \int_0^L \boldsymbol{\Delta}_j^T \boldsymbol{I}_0 \boldsymbol{\Delta}_i \, \mathrm{d}y = 0 \tag{29a}$$

or

$$\begin{aligned}
\int_0^L \boldsymbol{\Delta}_j^T \boldsymbol{I}_0 \boldsymbol{\Delta}_i \, \mathrm{d}y &= 0, \qquad \text{when} \qquad i \neq j \\
&\neq 0, \qquad \text{when} \qquad i = j
\end{aligned} \tag{29b}$$

Through the normalization, Eq. (29b) can be combined into

$$\int_0^L \boldsymbol{\Delta}_j^T \boldsymbol{I}_0 \boldsymbol{\Delta}_i \, \mathrm{d}y = \delta_{ij} \tag{30}$$

Expansion of Eq. (30) leads to

$$\begin{aligned}
\int_0^L &\left[m V_{0_i} V_{0_j} + m W_{f_i} W_{f_j} + I_y \Theta_i \Theta_j + I_x B_{f_i} B_{f_j}\right. \\
&+ I_{x^2 z^2} B_{r_i} B_{r_j} - m x_c \left(\Theta_i W_{f_j} + W_{f_i} \Theta_j\right) \\
&+ m z_c \left(B_{f_i} V_{0_j} + V_{0_i} B_{f_j}\right) + I_{xz} \left(B_{r_i} V_{0_j} + V_{0_i} B_{r_j}\right) \\
&\left. + I_{xz^2} \left(B_{r_i} B_{f_j} + B_{f_i} B_{r_j}\right)\right] \mathrm{d}y = \delta_{ij}
\end{aligned} \tag{31}$$

Unlike the usual orthogonality conditions where only the lateral deflection is considered, the orthogonality found in Eq. (31) shows that the complete set includes not only the mode shapes of the deflection but also the mode shapes of all of the other basic functions.

Forced Vibration

After finding the orthogonality relation (31), the expansion theorem may be used to obtain the system response by modal analysis. Using the expansion theorem, we write the solution of Eq. (14) as a superposition of the natural modes $\boldsymbol{\Delta}(y)$ multiplying corresponding time-dependent generalized coordinates $\eta_j(t)$. Hence,

$$\boldsymbol{\delta}(y, t) = \sum_{j=1}^{\infty} \boldsymbol{\Delta}_j(y) \eta_j(t) \tag{32}$$

and introducing Eq. (32) into Eq. (14), we obtain

$$\begin{aligned}
&\sum_{j=1}^{\infty} \left\{\left[\boldsymbol{K}_2 \boldsymbol{\Delta}_j''(y) + \left(\boldsymbol{K}_1 - \boldsymbol{K}_1^T\right)\boldsymbol{\Delta}_j'(y) - \boldsymbol{K}_0 \boldsymbol{\Delta}_j(y)\right]\eta_j(t)\right\} \\
&\quad + \boldsymbol{p}(y, t) = \boldsymbol{I}_0 \sum_{j=1}^{\infty} \boldsymbol{\Delta}_j(y) \ddot{\eta}_j(t)
\end{aligned} \tag{33}$$

Employing the results of Eq. (19) in Eq. (33), we get

$$\sum_{j=1}^{\infty} \left\{-\omega_j^2 \boldsymbol{I}_0 \boldsymbol{\Delta}_j(y) \eta_j(t)\right\} + \boldsymbol{p}(y, t) = \boldsymbol{I}_0 \sum_{j=1}^{\infty} \boldsymbol{\Delta}_j(y) \ddot{\eta}_j(t) \tag{34}$$

Multiplying both sides of Eq. (34) by $\boldsymbol{\Delta}_i^T(y)$, integrating over the spanwise length L, and utilizing the orthogonality relation (30), we obtain an infinite set of uncoupled second-order ordinary differential equations as

$$\ddot{\eta}_j(t) + \omega_j^2 \eta_j(t) = N_j(t), \qquad j = 1, 2, \ldots \tag{35a}$$

where $N_j(t)$ is a generalized force associated with the generalized coordinate $\eta_j(t)$ and is related to the load vector $\boldsymbol{p}$ by

$$N_j(t) = \int_0^L \boldsymbol{\Delta}_j^T(y) \boldsymbol{p}(y, t) \, \mathrm{d}y \tag{35b}$$

To solve the generalized coordinate $\eta_j(t)$ through the uncoupled second-order ordinary differential equation (35), we need to know the initial value of $\eta_j(t)$ and $\dot{\eta}_j(t)$. From relation (32) and the orthogonality condition (30), we have

$$\begin{aligned}
\eta_j(0) &= \int_0^L \boldsymbol{\Delta}_j^T(y) \boldsymbol{I}_0 \boldsymbol{\delta}(y, 0) \, \mathrm{d}y \\
\dot{\eta}_j(0) &= \int_0^L \boldsymbol{\Delta}_j^T(y) \boldsymbol{I}_0 \dot{\boldsymbol{\delta}}(y, 0) \, \mathrm{d}y
\end{aligned} \tag{36}$$

IV. Numerical Results and Discussion

Because the displacement fields assumed in Eq. (1) are quite general, to the authors' knowledge no analytical solution for the vibration analysis has been provided in the literature. However, several special conditions, such as those presented in the Appendix, have been widely discussed in the literature. Therefore, in this section we will first check our solutions by comparison with the existing numerical solutions for some special cases that can be reduced from our general formulations. After the verification through the known results, we will check the assumptions that the in-plane and rotary inertia terms can be disregarded for the cases of absence of in-plane spanwise loads. When these basic checks are done, we illustrate the numerical results of the natural frequencies and mode shapes of a NACA 2412 composite wing. From this case, we will then study some influential factors, such as transverse shear deformation, warping restraint, shape of airfoil, etc. Finally, through the analysis for the forced vibration presented, applications to the vibration suppression of composite wing will also be illustrated.

Table 1 Natural frequencies of a bending–torsion coupled cantilever composite beam

Mode	Frequency, Hz			
	Experimental[26]	Analytical[27]	Analytical[5]	Present
1	4.3	4.66	4.66	4.66
2	28	29.60	29.17	29.19
3	78	84.89	81.63	81.58
4	135	113.43	113.28	113.64
5	——	——	——	159.44

Table 2 Natural frequencies of a cantilever composite sandwich beam

Mode	Frequency, Hz	
	Hwu et al.[28]	Present
1	43.6	43.6
2	259.6	259.5
3	676.3	676.2
4	1212.3	1212.3
5	1822.4	1822.3

Table 3 Natural frequencies of a NACA 2412 composite wing

Method	Frequency, Hz				
	Mode 1	Mode 2	Mode 3	Mode 4	Mode 5
			$AR=8$		
Model (13)	16.15	96.37	110.34	252.10	333.79
Model (16)	16.15	96.45	110.34	252.45	333.85
FEM	15.75	93.84	114.94	245.18	343.82
			$AR=6$		
Model (13)	28.52	148.05	165.02	414.98	450.86
Model (16)	28.51	148.04	164.83	414.21	450.71
FEM	27.90	154.10	160.47	403.10	459.12
			$AR=4$		
Model (13)	63.00	225.71	336.39	690.77	790.67
Model (16)	62.97	225.69	335.69	690.42	788.67
FEM	61.88	233.57	326.95	686.14	765.56
			$AR=2$		
Model (13)	230.66	470.18	970.81	1446.6	2031.5
Model (16)	230.39	470.07	966.74	1443.6	2030.7
FEM	227.36	475.58	938.53	1325.8[a]	1468.1[a]

[a]Natural frequencies by FEM from fourth to seventh modes are 1325.8, 1468.1, 1983.9, and 2029.8, respectively.

Comparison with Existing Numerical Solutions for Some Special Cases

Example 1: Bending–Torsion Coupled Cantilever Composite Beam

To compare with the results presented in the literature, the laminate layup $[45/0]_{3s}$, geometry, and its associated material properties are extracted from Ref. 5 as $L=0.56$ m, $W=0.03$ m, $h=0.018$ m, $\rho=136.722$ kg/m^3, $\tilde{D}_{22}=0.5317$ N·m^2, $\tilde{D}_{66}=0.08965$ N·m^2, and $\tilde{D}_{26}=0.0495$ N·m^2 where in conventional terms $\tilde{D}_{22}=EI$, $4\tilde{D}_{66}=GJ$, and $2\tilde{D}_{26}=K$ are the bending rigidity, torsional rigidity, and bending–torsion coupling rigidity, respectively. In Ref. 5, the transverse shear deformation is neglected, and the free warping condition is assumed, that is, $\gamma_{yz}=0$ and $\lambda=0$, which is discussed in the first and second subsections of the Appendix. Table 1 shows that our results for the natural frequencies agree well with the existing experimental and analytical solutions.[5,26,27]

Example 2: Cantilever Composite Sandwich Beam

In the preceding example, the bending–torsion coupling is considered, but transverse shear deformation is neglected. To check our results for the consideration of the transverse shear deformation, we now consider a composite sandwich beam $[0_2/90_2/0_2/\text{core}]_s$ whose geometry and material properties are[28] $L=0.7112$ m, $h_f=0.2286$ mm, and $h_c=12.7$ mm. For the face, $\rho_f=1480$ kg/m^3, $E_L=130$ GPa, $E_T=10$ GPa, $G_{LT}=4.85$ GPa, and $\nu_{LT}=0.25$. For the core, $\rho_c=32.8$ kg/m^3 and $G_{xz}=0.08274$ GPa. In this case, the torsion and the rate of angle change are neglected, that is, $\theta=\beta_r=0$, which is discussed in the third subsection of the Appendix. Table 2 shows that our results are almost the same as those presented in Ref. 28.

Vibration Analysis for NACA 2412 Composite Wing

After verifying our results by using the flat composite beam model, we now consider a composite wing structure with a NACA 2412 airfoil. From the data given in Ref. 29, the shape of airfoil can be approximated by a ninth-order polynomial as

$$f_u(\bar{x})/c = 0.0719 - 0.0588\bar{x} - 0.0769\bar{x}^2 - 0.767\bar{x}^3 - 2.599\bar{x}^4 + 15.382\bar{x}^5 + 18.536\bar{x}^6 - 92.174\bar{x}^7 - 45.673\bar{x}^8 + 186.078\bar{x}^9$$

$$f_u(\bar{x})/c = -0.0329 + 0.0405\bar{x} - 0.0239\bar{x}^2 + 0.675\bar{x}^3 + 1.815\bar{x}^4 - 12.310\bar{x}^5 - 13.870\bar{x}^6 + 73.449\bar{x}^7 + 36.096\bar{x}^8 - 149.862\bar{x}^9$$

$$\bar{x} = x/c$$

where $f_u(\bar{x})$ and $f_l(\bar{x})$ are the approximate functions for the upper and lower surfaces of the airfoil, respectively, in which the coordinate origin is located at the midpoint of the chord line. The wing chordwise length $c=0.1$ m and spanwise length $L=0.4$ m. The wing skin is made of a graphite/epoxy fiber-reinforced composite whose mechanical properties are $E_L=200$ GPa, $E_T=5$ GPa, $\nu_{LT}=0.25$, $G_{LT}=2.5$ GPa, and $\rho=1.9$ g/cm^3 with ply thickness $t=0.025$ mm. The laminate layup is [90/−45/45/0] for upper skin and [0/45/−45/90] for lower skin. Two wing spars made of isotropic materials with shear modulus $G=8$ GPa and thickness 0.6 mm are located at $\pm 0.25c$ from the midchord line. Eight stringers and two ribs, made of aluminum with material properties $E=69$ GPa, $\nu=0.33$, $G=26$ GPa, $\rho=2.8$ g/cm^3, are equally spaced on the wing as shown in Fig. 2.

Before performing the vibration analysis for the cases where the in-plane spanwise surface loads are absent, we check the assumptions that the in-plane and rotary inertia terms $m\ddot{v}_0$, $mz_c\ddot{\beta}_f$, and $I_{xz}\ddot{\beta}_r$ are disregarded. Table 3 shows a comparison of the natural frequencies obtained from the most general model characterized by Eqs. (13) with that of the absence of in-plane spanwise loads characterized by Eqs. (16) and shows that all of their differences are below 0.5%, which means that the assumptions made for the case of absence of in-plane spanwise loads are reasonable and acceptable. The results also show a physically reasonable tendency that the larger the aspect ratio is, the smaller the natural frequency becomes. With this confidence, all of the following examples are done by the equivalent eigth-order system of equations made for the case of absence of in-plane spanwise loads. Based on this equivalent reduced model, the first three modal shapes of NACA 2412 composite wing with $AR=8$ are shown in Figs. 3a–3c. By using the values shown in Figs. 3a–3c, one may construct the three-dimensional modal shapes through the displacement fields assumed in Eq. (1). With the present two-dimensional plots for bending W_f, torsion Θ, rotation B_f, and angle rate B_r, we observe that unlike the simple beam theory no pure bending or torsional mode occurs in the first three natural modes, which are all coupled modes.

To further validate for the present model, Table 3 also shows the comparison of the natural frequencies with those obtained from the commercial finite element software ANSYS, and the results agree well with each other. In Table 3, the finite element model (FEM) indicates the analysis by ANSYS in which the composite wing is modeled as a multilayered shell with nonuniform thickness in the shape of the NACA 2412 airfoil. Just as our model, the stringers and spar flanges are modeled as a pseudolamina whose equivalent moduli are evaluated by Eq. (10), and the spar webs and ribs are modeled as a core whose equivalent moduli are evaluated by Eq. (11). With these equivalent moduli and the moduli of laminated skins, the material properties of the shells can be input layer by layer. To have a compatible degree of freedom with our present model, the element used for the analysis is selected to be SHELL91. The

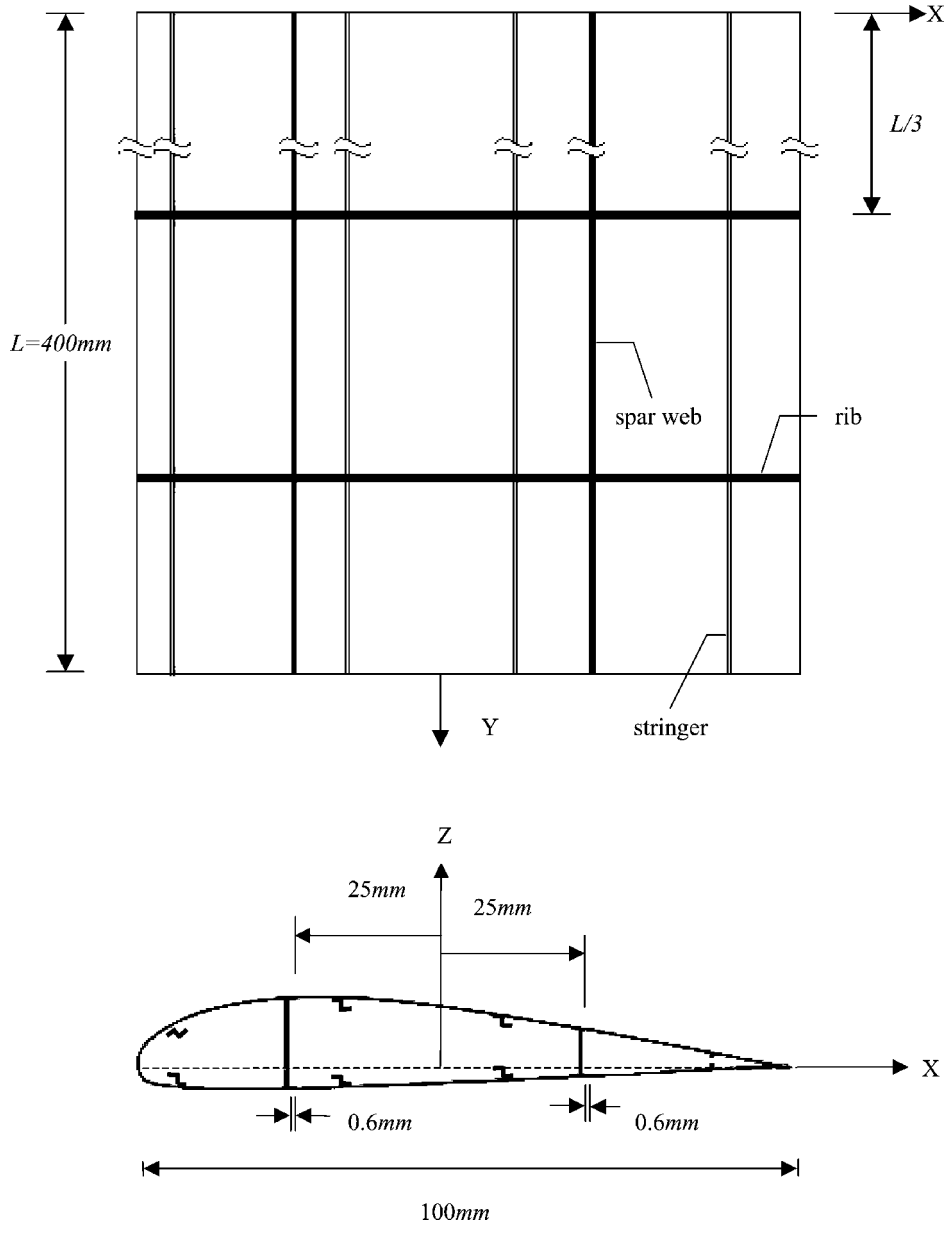

Fig. 2 Arrangement of NACA 2412 composite wing.

boundary conditions are given by fixing all nodes at the wing root and restricting the movement of all nodes in the x direction, that is, $u_0 = 0$, as described in Eq. (1). After the convergence studies for the element meshes, 2000 elements and 6241 nodes for $AR = 2$, 4000 elements and 12281 nodes for $AR = 4$, 6000 elements and 18,321 nodes for $AR = 6$, and 8000 elements and 24,361 nodes for $AR = 8$ are used in the analysis. Note that when $AR = 2$, a small discrepancy between the present model and FEM occurs for the natural frequencies of modes 4 and 5. By checking their following natural frequencies and associated mode shapes, we found that in this case our mode 4 corresponds to FEM's mode 5, and our mode 5 corresponds to FEM's mode 7.

Studies of Some Influential Factors

Example 1: Effect of Transverse Shear Deformation

From Eq. (11) we know that the equivalent transverse shear modulus of the composite wing considered in this paper is related to the shear modulus and section area of the spar webs. The effects of transverse shear deformation can, therefore, be studied by varying the properties of spar webs and all of the other properties given previously for the NACA 2412 composite wing remain the same. Figure 4 shows the effect of the equivalent transverse shear modulus on the natural frequency of the first mode. From Fig. 4, we see that the larger the transverse shear modulus, the higher the natural frequency, and after a certain value of G_{yz} (about 0.1 GPa for $AR = 4$, 6, and 8 and about 1 GPa for $AR = 2$) the natural frequency will approach to a constant value, which is exactly the one obtained by neglecting the transverse shear deformation. This is reasonable because the neglect of the transverse shear deformation means that its corresponding modulus is assumed to be infinite. Figure 4 also shows that the influence of the transverse shear modulus is more pronounced when the aspect ratio is smaller. As to the effects of transverse shear modulus on the natural frequencies of higher modes, similar figures have been plotted in Ref. 30. These results show that consideration of transverse shear deformation is important for the wing structures with equivalent shear modulus less than 1 GPa.

Example 2: Effect of Warping Restraint

As discussed in the second subsection of the Appendix, the inclusion of the warping restraint effects can be achieved by letting $\lambda = 1$, whereas the free-warping condition is denoted by $\lambda = 0$. When the fixed end is relaxed and free warping is allowed, it is reasonable to

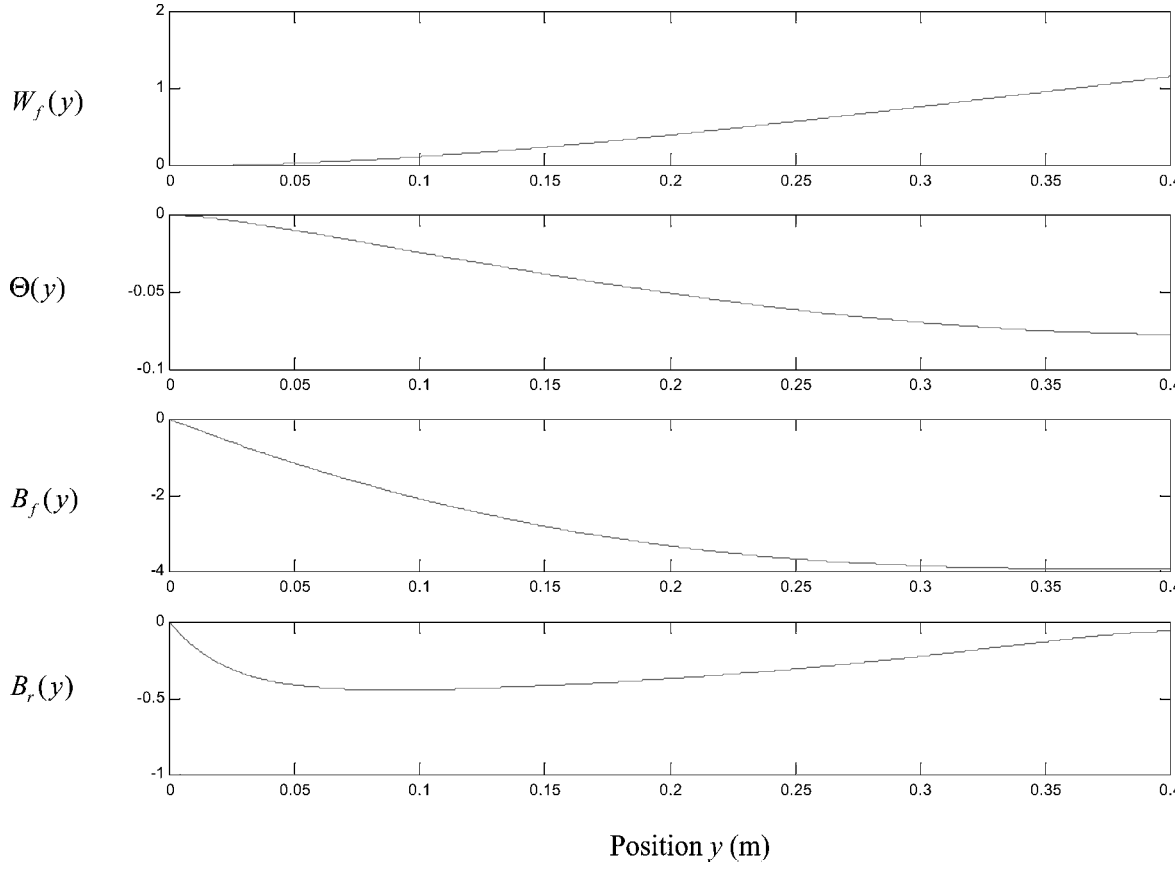

a)

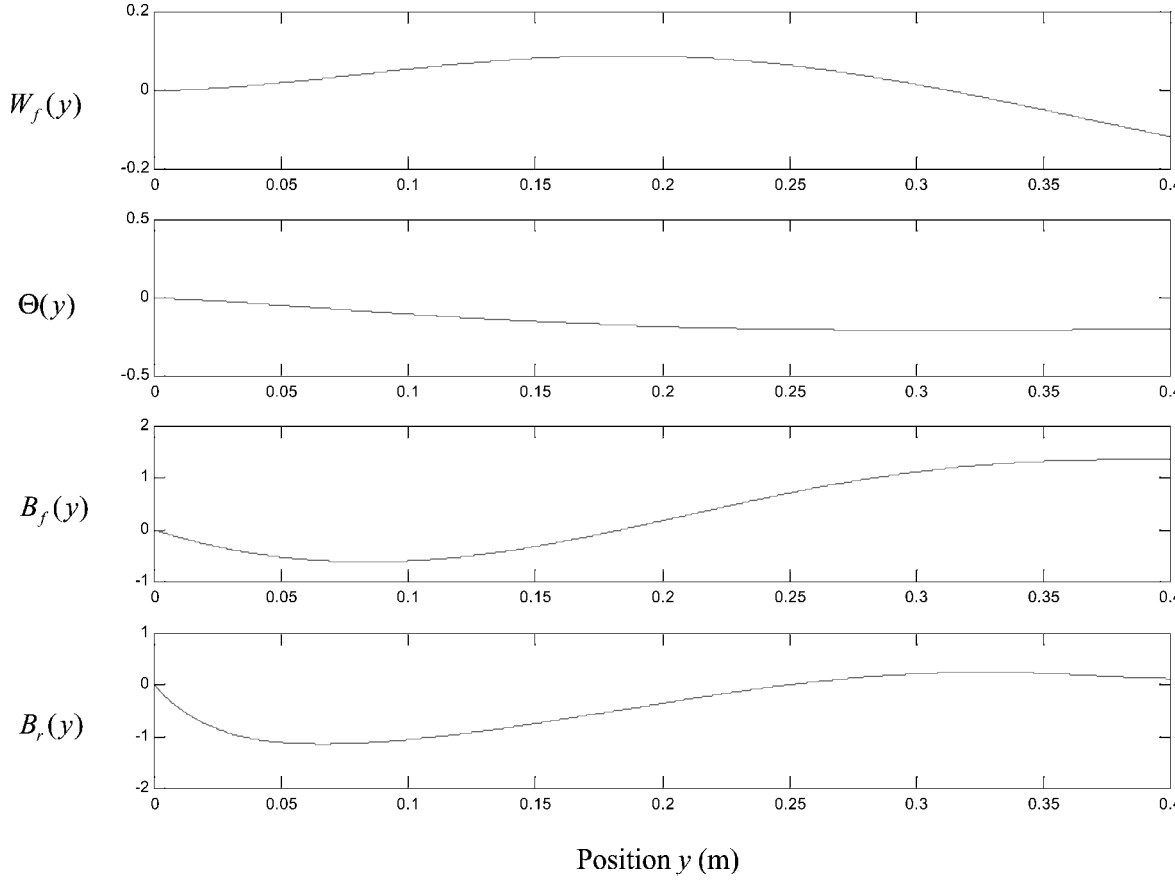

b)

Fig. 3 Mode shapes of NACA 2412 composite wing ($AR = 8$): a) first mode, b) second mode, and c) third mode.

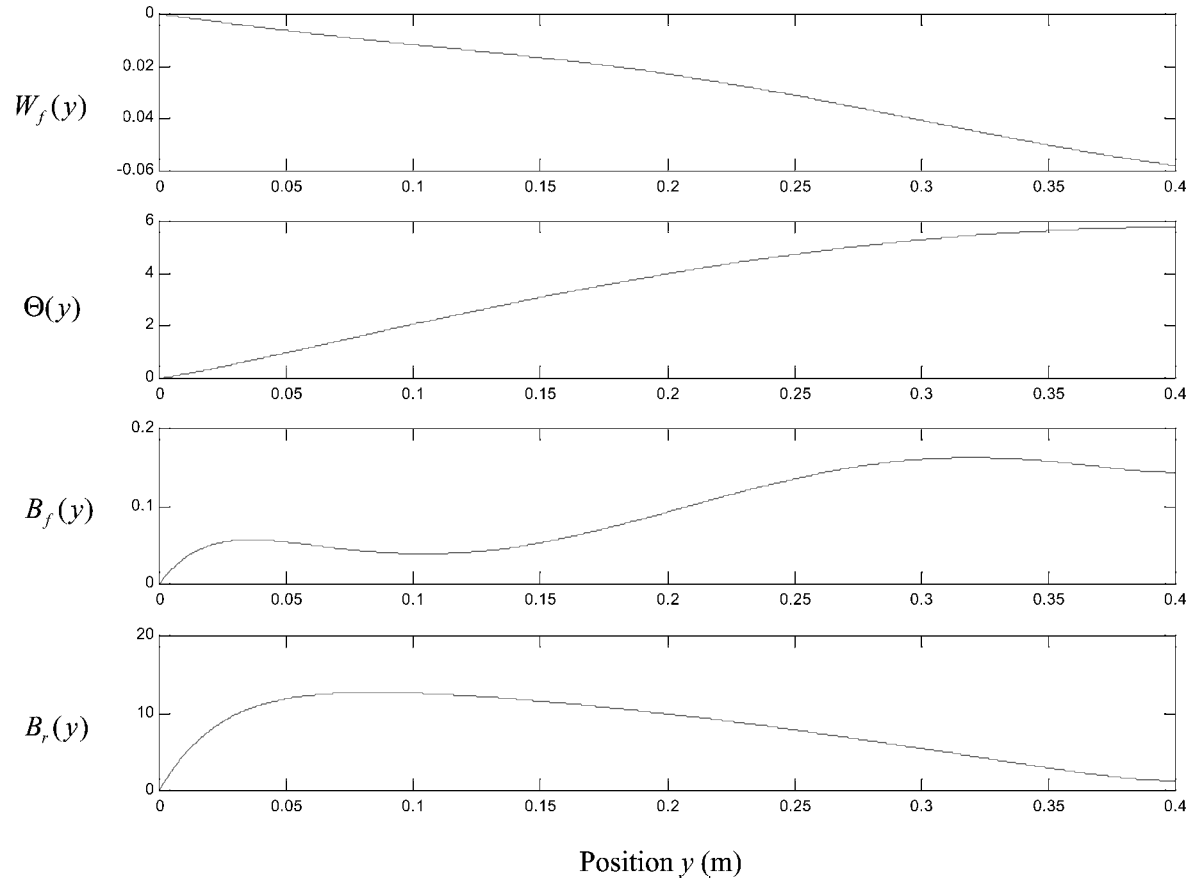

c)

Fig. 3 Mode shapes of NACA 2412 composite wing ($AR = 8$): a) first mode, b) second mode, and c) third mode (continued).

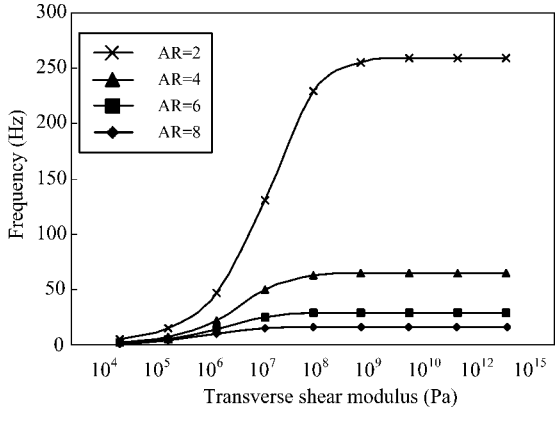

Fig. 4 Natural frequencies vs transverse shear modulus for several different aspect ratios (first mode).

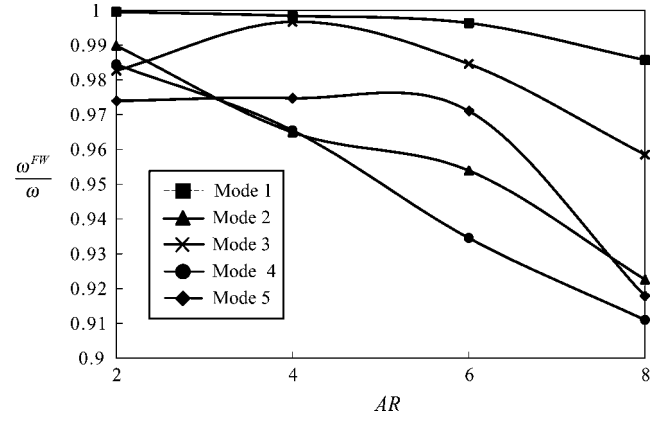

Fig. 5 Effects of free warping on the natural frequencies of the first five modes.

expect that the composite wing will behave softer and its natural frequencies will then become smaller, that is, the ratio $\omega^{\mathrm{FW}}/\omega$ should be less than one. The warping restraint effects can, therefore, be studied from the variation of this ratio. Figure 5 show that $0.9 < \omega^{\mathrm{FW}}/\omega < 1$ for the first five modes with aspect ratio ranging from 2 to 8. The results also show that the higher the aspect ratio, the lower $\omega^{\mathrm{FW}}/\omega$, which means that the more slender the wing is, the more influential the warping restraint effects are.

Example 3: Effect of Airfoil Shape

To study the effect of airfoil shape, we consider an approximation by the third-order polynomial where the mean square error with respect to the actual airfoil is 4.7% (Ref. 18), whereas that of the ninth-order polynomial shown previously is 0.048%. Table 4 shows that the first five natural frequencies obtained from these two different airfoil shapes for $AR = 6$ and 8 differ from 10 to 28%, which means that a 4.7% error of shape approximation may lead to 28% error of natural frequency. If the error of approximation is restricted to within 0.4%, the corresponding error of natural frequency will be under 1.4% (Ref. 30). In other words, the approximation of the airfoil shape within a error tolerance such as 0.4% is important to obtain accurate natural frequencies with errors under 1.4%.

Applications to Vibration Suppression of Composite Wing

In previous examples, only the free vibration analysis is considered. To illustrate the capability of our general model for the forced vibration analysis, we now focus our attention to the uncoupled second-order differential equation system (35). Because

Table 4 Effects of airfoil shape on the natural frequencies

Mode	Frequency, Hz: Ninth-order polynomial	Frequency, Hz: Third-order polynomial	Error, %
	AR = 8		
1	16.1	18.7	15.6
2	96.4	110.1	14.2
3	110.3	140.4	27.2
4	252.4	283.5	12.3
5	333.9	421.9	26.4
	AR = 6		
1	28.5	32.9	15.4
2	148.1	186.0	25.7
3	165.0	187.8	13.8
4	415.0	459.1	10.6
5	450.9	564.2	25.1

this equation system is exactly the same as that of simple beam theory, the same approach for the forced vibration analysis can be applied to the present model. A typical and useful example for the forced vibration analysis is the vibration suppression. In our previous study,[28] an LQG/LTR controller is designed for the composite sandwich beams by bonding piezoelectric sensors and actuators on the beam surfaces. Because the governing equation system (35) for the generalized coordinate $\eta_j(t)$ is exactly the same as that of the composite sandwich beams discussed in Ref. 28, to save space, we will not present the derivation of the sensor equation, the actuator equation, and the dynamics of the observed-state feedback control system. Only the numerical simulation for the vibration suppression of composite wing is shown in Figs. 6a and 6b. From Figs. 6a and 6b we see that based on the vibration analysis model developed in this paper the LQG/LTR controller successfully suppresses the vibration of composite wing within 4 s. More detailed discussions and illustrations may be found in Ref. 30.

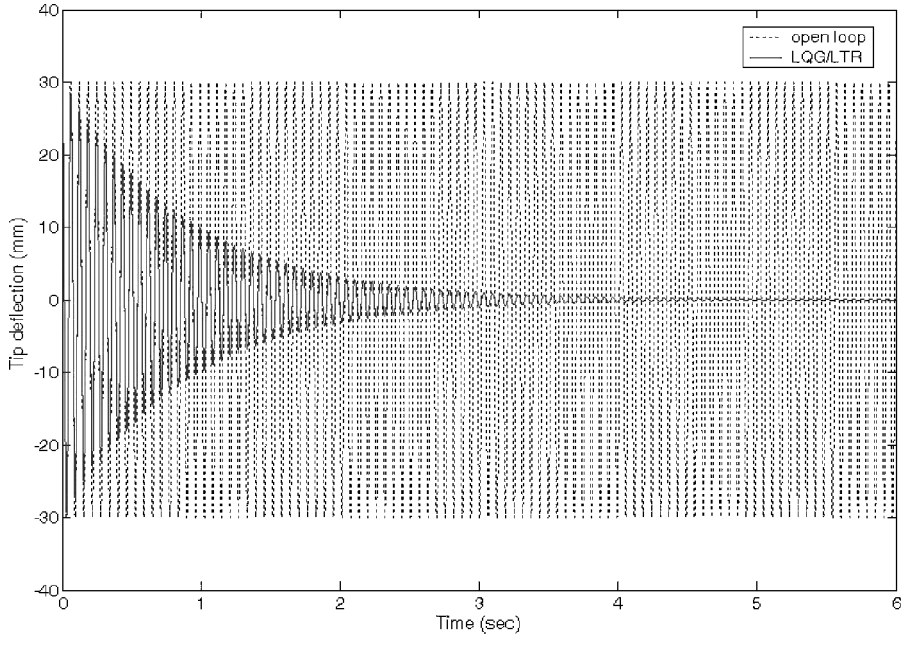

a)

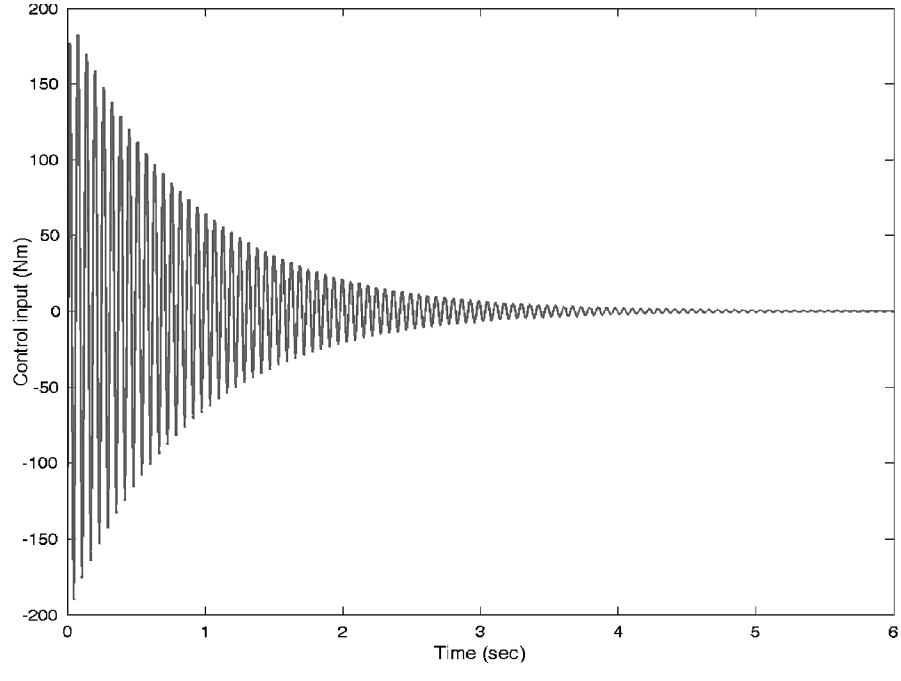

b)

Fig. 6 Vibration suppression of NACA 2412 composite wing with first mode initial condition: a) tip deflection response and b) control input force.

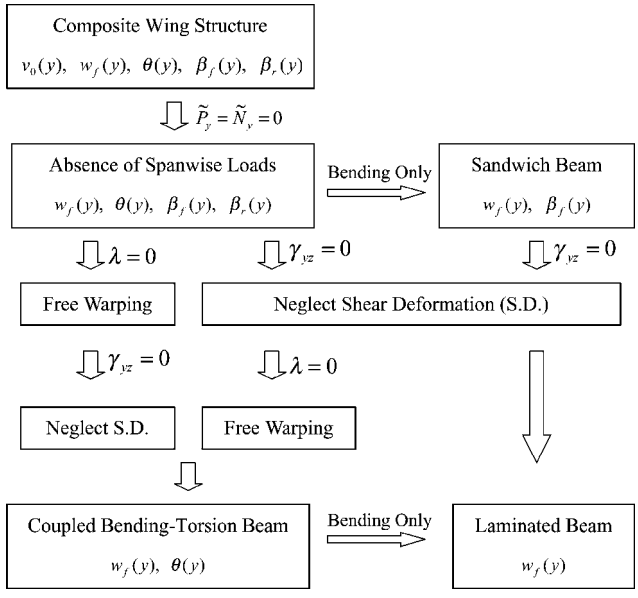

Fig. 7 Connection among several different composite wing models.

General Discussion

Because the comprehensive model presented in this paper is quite general and can cover several different simplified models considered in the literature, to show clearly the connection between the present model and those simplified models, a flowchart is given in Fig. 7. From Fig. 7, we see that due to the introduction of the five basic functions v_0, w_f, θ, β_f, and β_r, the present model incorporates various effects such as bending–torsion coupling, warping restraint, transverse shear deformation, shape of airfoil, rotary inertia, etc. Most of the models discussed in the literature can then be simplified with the present model, such as the coupled bending–torsion beam (w_f, θ), sandwich beam (w_f, β_f), and laminated beam (w_f) shown in Fig. 7.

V. Conclusions

When the matrix form representation is used, the vibration analysis shown in Sec. III becomes simple and elegant. Many equations if written in scalar form may be very complicated and are not easily solved analytically. With matrix form representation, most of the equations have the same form as those of classical beam theory, for example, the governing equation (14), the boundary conditions (15), the orthogonality condition (30), and the uncoupled second-order differential equation (35). Without using the matrix form representation, some relations cannot even be found by direct scalar form derivation, such as the scalar form of the orthogonality condition (31). If the orthogonality condition is lost, it is almost impossible to get the simple uncoupled second-order differential equation system shown in Eq. (35) for forced vibration analysis.

To show the accuracy and generality of the present model, several different examples are given. Our solutions first compare well, with the existing numerical solutions for some special cases, then the preassumptions made for the cases of absence of spanwise loads compare well, and finally compare well with commercial finite element solutions for a NACA 2412 composite wing. After these basic checks, some influential factors are studied and the numerical results show that 1) the larger the transverse shear modulus, the higher the natural frequency and that after a certain value of G_{yz} the natural frequency will approach to a constant value, which is exactly the one obtained by neglecting the transverse shear deformation; 2) the more slender the wing, the more influential the warping restraint effects; and 3) the approximation of the airfoil shape within a tolerant error is important for obtaining the accurate natural frequencies. Finally, based on the vibration analysis model developed in this paper a LQG/LTR controller with piezoelectric sensors and actuators bonded on the wing surfaces is designed and proved to be successful for vibration suppression of a composite wing.

Appendix: Special Considerations of Dynamic Modeling

Neglect of the Transverse Shear Deformation ($\gamma_{yz} = 0 \Rightarrow \beta_f = -w_f', \beta_r = \theta'$)

Usually when the plate thickness is thin enough or the transverse shear modulus is large enough, the transverse shear deformation may be neglected, that is, $\gamma_{yz} = 0$, and the problem formulation may be further simplified. Although this is generally not true for the wing structures considered in this paper, here we make this simplification just for the purpose of comparison with some simplified models presented in the literature such as in Ref. 7. From Eq. (2) we see that $\gamma_{yz} = 0$ may lead to $\beta_f = -w_f'$ and $\beta_r = \theta'$. With these two relations for the cases of absence of in-plane spanwise loads, the number of the independent functions will only remain two, that is, w_f and θ. The equations of motion corresponding to the deflection w_f and the slope θ can then be obtained by substituting Eq. (4d) into Eq. (4b) and Eq. (4e) into Eq. (4c) with $\beta_f = -w_f'$ and $\beta_r = \theta'$. If the distributed moments $\tilde{m}_x$, $\tilde{m}_y$, and $\tilde{m}_y^*$ are neglected, the results are

$$\frac{\partial^2 \tilde{M}_y}{\partial y^2} + \tilde{p} = m\ddot{w}_f - mx_c\ddot{\theta}$$

$$2\frac{\partial \tilde{M}_{xy}}{\partial y} - \lambda\frac{\partial^2 \tilde{M}_y^*}{\partial y^2} = \tilde{p}^* - mx_c\ddot{w}_f + I_y\ddot{\theta} \tag{A1}$$

Their associated boundary conditions become

$$\tilde{M}_y' = \hat{\tilde{M}}_y', \qquad \text{or} \qquad w_f = \hat{w}_f$$

$$2\tilde{M}_{xy} - \lambda\tilde{M}_y^{*'} = 2\hat{\tilde{M}}_{xy} - \lambda\hat{\tilde{M}}_y^{*'}, \qquad \text{or} \qquad \theta = \hat{\theta}$$

$$\tilde{M}_y = \hat{\tilde{M}}_y, \qquad \text{or} \qquad w_f' = \hat{w}_f'$$

$$\lambda\tilde{M}_y^* = \lambda\hat{\tilde{M}}_y^*, \qquad \text{or} \qquad \lambda\theta' = \lambda\hat{\theta}' \tag{A2}$$

Employment of the constitutive relations (13b) with Eqs. (16c) and (16d) into Eqs. (A1) and (A2) now gives us the governing equations and the boundary conditions as

$$2\bar{D}_{26}\theta''' - \left[\bar{D}_{22}w_f'' - \lambda\bar{D}_{22}^*\theta''\right]'' - m\ddot{w}_f + mx_c\ddot{\theta} + \tilde{p} = 0$$

$$4\bar{D}_{66}\theta'' - 2\bar{D}_{26}w_f''' + \lambda\left[\bar{D}_{22}^*w_f'' - \lambda\bar{D}_{22}^{**}\theta''\right]'' + mx_c\ddot{w}_f - I_y\ddot{\theta} - \tilde{p}^* = 0 \tag{A3}$$

$$2\bar{D}_{26}\theta'' - \bar{D}_{22}w_f''' + \lambda\bar{D}_{22}^*\theta''' = \hat{\tilde{M}}_y', \qquad \text{or} \qquad w_f = \hat{w}_f$$

$$4\bar{D}_{66}\theta' - 2\bar{D}_{26}w_f'' + \bar{D}_{22}^*\lambda w_f''' - \bar{D}_{22}^{**}\lambda\theta''' = 2\hat{\tilde{M}}_{xy} - \lambda\hat{\tilde{M}}_y^{*'} \qquad \text{or} \qquad \theta = \hat{\theta}$$

$$2\bar{D}_{26}\theta' - \bar{D}_{22}w_f'' + \bar{D}_{22}^*\lambda\theta'' = \hat{\tilde{M}}_y, \qquad \text{or} \qquad w_f' = \hat{w}_f'$$

$$\lambda\left[2\bar{D}_{26}^*\theta' - \bar{D}_{22}^*w_f'' + \bar{D}_{22}^{**}\theta''\right] = \lambda\hat{\tilde{M}}_y^*, \qquad \text{or} \qquad \lambda\theta' = \lambda\hat{\theta}' \tag{A4}$$

Neglect of the Warping Restraint Effects ($\varepsilon_y = v_0' + z\beta_f' \Rightarrow \lambda = 0$)

The importance of the warping restraint effects has been discussed in works such as Ref. 8. As mentioned in Sec. II, the inclusion of the warping restraint effect can be achieved by letting $\lambda = 1$. On the other hand, $\lambda = 0$ denotes the free-warping condition. When $\lambda = 0$ is substituted into the governing equations (14) with absence of in-plane spanwise loads, it can be observed that β_r is no longer an independent function, but is a dependent function of w_f, θ, and β_f. Thus, the system of governing equations may be further reduced from eigth order to sixth order.

Reduction to the Conventional Composite Sandwich Beams ($\theta = \beta_r = 0$)

The difference of the present model with the conventional composite sandwich beams is the consideration of the torsional angle θ and the rate of angle change β_r. If we neglect these two variations, the formulations should be exactly the same as those of conventional composite sandwich beams. Substituting $\theta = \beta_r = 0$ into the equations of motion (4b) and (4d) corresponding to the deflection w_f and rotation β_f, we get

$$\frac{\partial \tilde{Q}_y}{\partial y} + \tilde{p} = m\ddot{w}_f, \qquad \frac{\partial \tilde{M}_y}{\partial y} = \tilde{Q}_y + I_x\ddot{\beta}_f \tag{A5}$$

Their associated boundary conditions are

$$\tilde{Q}_y = \hat{\tilde{Q}}_y, \qquad \text{or} \qquad w_f = \hat{w}_f$$

$$\tilde{M}_y = \hat{\tilde{M}}_y, \qquad \text{or} \qquad \beta_f = \hat{\beta}_f \tag{A6}$$

Use of the constitutive relations will then provide the governing equations

$$\tilde{A}_{44}\beta_f' + \tilde{A}_{44}w_f'' - m\ddot{w}_f + \tilde{p} = 0$$

$$\tilde{A}_{44}\beta_f + \tilde{A}_{44}w_f' - \bar{D}_{22}\beta_f'' + I_x\ddot{\beta}_f = 0 \tag{A7}$$

and the boundary conditions

$$\tilde{A}_{44}(\beta_f + w_f') = \hat{\tilde{Q}}_y, \qquad \text{or} \qquad w_f = \hat{w}_f$$

$$\bar{D}_{22}\beta_f' = \hat{\tilde{M}}_y, \qquad \text{or} \qquad \beta_f = \hat{\beta}_f \tag{A8}$$

Reduction to the Conventional Laminated Beams ($\theta = \beta_r = 0$, $\beta_f = -w_f'$, $I_x = 0$)

When the thickness of the laminated beam is considered to be much smaller relative to its length, the transverse shear deformation and the rotary inertia are usually ignored, that is, $\gamma_{yz} = 0$ and $I_x = 0$, in which the former leads to $\beta_f = -w_f'$. Substituting $\beta_f = -w_f'$ and $I_x = 0$ into Eqs. (A5–A8) may now provide the equation of motion and its associated boundary conditions as

$$\frac{\partial^2 \tilde{M}_y}{\partial y^2} + \tilde{p} = m\ddot{w}_f \Rightarrow \left[\bar{D}_{22}w_f''\right]'' + m\ddot{w}_f - \tilde{p} = 0 \tag{A9}$$

$$\tilde{M}_y' = -\bar{D}_{22}w_f''' = \hat{\tilde{M}}_y', \qquad \text{or} \qquad w_f = \hat{w}_f$$

$$\tilde{M}_y = -\bar{D}_{22}w_f'' = \hat{\tilde{M}}_y, \qquad \text{or} \qquad w_f' = \hat{w}_f' \tag{A10}$$

Acknowledgments

The authors thank the National Science Council (NSC) for support through grant NSC 89-2212-E-006-192, NSC 90-2212-E-006-173 and NSC 91-2212-E-006-125. They also thank S. H. Cheng for running the NACA example by using the finite element software ANSYS.

References

[1]Bisplinghoff, R. L., Asheley, H., and Halfman, R. L., *Aeroelasticity*, Addison–Wesley, Cambridge, MA, 1955, Chaps. 2 and 3.

[2]Megson, T. H. G., *Aircraft Structures—for Engineering Students*, 2nd ed., Edward Arnold, London, 1990, Chap. 8.

[3]Weisshaar, T. A., and Foist, B. L., "Vibration Tailoring of Advanced Composite Lifting Surfaces," *Journal of Aircraft*, Vol. 22, 1985, pp. 141–147.

[4]Chandra, R., Stemple, A. D., and Chopra, I., "Thin-Walled Composite Beams Under Bending, Torsional, and Extensional Loads," *Journal of Aircraft*, Vol. 27, 1990, pp. 619–626.

[5]Banerjee, J. R., and Williams, F. W., "Free Vibration of Composite Beams: An Exact Method Using Symbolic Computation," *Journal of Aircraft*, Vol. 32, No. 3, 1995, pp. 636–642.

[6]Crawley, E. F., and Dugundji, J., "Frequency Determination and Nondimensionalization for Composite Cantilever Plates," *Journal of Sound and Vibration*, Vol. 72, No. 1, 1980, pp. 1–10.

[7]Lottati, I., "Flutter and Divergence Aeroelastic Characteristics for Composite Forward Swept Cantilevered Wing," *Journal of Aircraft*, Vol. 22, No. 11, 1985, pp. 1001–1007.

[8]Librescu, L., and Khdeir, A. A., "Aeroelastic Divergence of Swept-Forward Composite Wings Including Warping Restraint Effect," *AIAA Journal*, Vol. 26, No. 11, 1988, pp. 1373–1377.

[9]Oyibo, G. A., and Bentson, J., "Exact Solutions to the Oscillations of Composite Aircraft Wings with Warping Constraint and Elastic Coupling," *AIAA Journal*, Vol. 28, No. 6, 1990, pp. 1075–1081.

[10]Librescu, L., and Song, O., "On the Static Aeroelastic Tailoring of Composite Aircraft Swept Wings Modelled as Thin-Walled Beams Structures," *Composite Engineering*, Special Issue, Use of Composite in Rotor Craft and Smart Structures, Vol. 2, No. 5-7, 1992, pp. 497–512.

[11]Volovoi, V. V., and Hodges, D. H., "Single- and Multicelled Composite Thin-Walled Beams," *AIAA Journal*, Vol. 40, No. 5, 2002, pp. 960–965.

[12]Volovoi, V. V., and Hodges, D. H., "Theory of Anisotropic Thin-Walled Beams," *Journal of Applied Mechanics*, Vol. 67, No. 3, 2000, pp. 453–459.

[13]Yu, W., Volovoi, V. V., Hodges, D. H., and Hong, X., "Validation of the Variational Asymptotic Beam Sectional Analysis," *AIAA Journal*, Vol. 40, No. 10, 2002, pp. 2105–2112.

[14]Yu, W., Hodges, D. H., Volovoi, V. V., and Cesnik, C. E. S., "On Timoshenko-Like Modeling of Initially Curved and Twisted Composite Beams," *International Journal of Solids and Structures*, Vol. 39, 2002, pp. 5101–5121.

[15]Karpouzian, G., and Librescu, L., "Comprehensive Model of Anisotropic Composite Aircraft Wings Suitable for Aeroelastic Analyses," *Journal of Aircraft*, Vol. 31, No. 3, 1994, pp. 703–712.

[16]Johnson, E. R., Vasiliev, V. V., and Vasiliev, D. V., "Anisotropic Thin-Walled Beams with Closed-Sectional Contours," *AIAA Journal*, Vol. 39, No. 12, 2001, pp. 2389–2393.

[17]Jung, S. N., Nagaraj, V. T., and Chopra, I., "Refined Structural Model for Thin- and Thick-Walled Composite Rotor Blades," *AIAA Journal*, Vol. 40, No. 1, 2002, pp. 105–116.

[18]Hwu, C., and Tsai, Z. S., "Aeroelastic Divergence of Stiffened Composite Multicell Wing Structures," *Journal of Aircraft*, Vol. 39, No. 2, 2002, pp. 242–251.

[19]Hodges, D. H., "Review of Composite Rotor Blade Modeling," *AIAA Journal*, Vol. 28, No. 3, 1990, pp. 561–565.

[20]Jung, S. N., Nagaraj, V. T., and Chopra, I., "Assessment of Composite Rotor Blade Modeling Techniques," *Journal of the American Helicopter Society*, Vol. 44, No. 3, 1999, pp. 188–205.

[21]Volovoi, V. V., Hodges, D. H., Cesnik, C. E. S., and Popescu, B., "Assessment of Beam Modeling Methods for Rotor Blade Applications," *Mathematical and Computer Modelling*, Vol. 33, 2001, pp. 1099–1112.

[22]Hwu, C., and Hu, J. S., "Buckling and Postbuckling of Delaminated Composite Sandwich Beams," *AIAA Journal*, Vol. 30, No. 7, 1992, pp. 1901–1909.

[23]Hu, J. S., and Hwu, C., "Free Vibration of Delaminated Composite Sandwich Beams," *AIAA Journal*, Vol. 33, No. 10, 1995, pp. 1911–1918.

[24]Cowper, G. R., "The Shear Coefficient in Timoshenko's Beam Theory," *Journal of Applied Mechanics*, Vol. 3, No. 2, 1966, pp. 335–340.

[25]Meirovitch, L., *Dynamics and Control of Structures*, Wiley, New York, 1990, Chap. 7.

[26]Minguet, P., and Dugundji, J., "Experiments and Analysis for Composite Blades Under Large Deflections, Part 2: Dynamic Behavior," *AIAA Journal*, Vol. 28, No. 9, 1990, pp. 1580–1588.

[27]Hodges, D. H., Atilgan, A. R., Fulton, M. V., and Rehfield, L. W., "Free Vibration Analysis of Composite Beams," *Journal of the American Helicoper Society*, Vol. 36, 1991, pp. 36–47.

[28]Hwu, C., Chang, W. C., and Gai, H. S., "Vibration Suppression of Composite Sandwich Beams," *Journal of Sound and Vibration* (to be published).

[29]Hunsaker, J. C., *Theory of Wing Sections*, McGraw–Hill, New York, 1949, p. 410.

[30]Gai, H. S., "Vibration Analysis and Control of Composite Wing Structures," M.S. Thesis Inst. of Aeronautics and Astronautics, National Cheng-Kung Univ., Tainan, Taiwan, Republic of China, June 2002.

A. Berman
Associate Editor